Cystic Fibrosis Transmembrane Conductance Regulator (CFTR) Nucleotide-Binding Domain 1 (NBD-1) and CFTR Truncated within NBD-1 Target to the Epithelial Plasma Membrane and Increase Anion Permeability†

J. P. Clancy,*,‡,§ J. S. Hong,|| Z. Bebök,⊥ S. A. King,§ S. Demolombe,# D. M. Bedwell,§,▽ and E. J. Sorscher§,⊥

Departments of Cell Biology, Medicine, Microbiology and Pediatrics, Gregory Fleming James Cystic Fibrosis Research Center, University of Alabama at Birmingham, 1918 University Boulevard (782 MCLM), Birmingham, Alabama 35294, and University of Nantes Hospital G & R Laennec, BP 1005, 44035 Nantes, France

Received February 24, 1998; Revised Manuscript Received July 8, 1998

ABSTRACT: The cystic fibrosis transmembrane conductance regulator (CFTR) is a member of the traffic ATPase family that includes multiple proteins characterized by (1) ATP binding, (2) conserved transmembrane (TM) motifs and nucleotide binding domains (NBDs), and (3) molecular transport of small molecules across the cell membrane. While CFTR NBD-1 mediates ATP binding and hydrolysis, the membrane topology and function of this domain in living eukaryotic cells remains uncertain. In these studies, we have expressed wild-type CFTR NBD-1 (amino acids 433−586) or NBD-1 containing the ΔF508 mutation transiently in COS-7 cells and established that the domain is situated across the plasma membrane by four independent assays; namely, extracellular chymotrypsin digestion, surface protein biotinylation, confocal immunofluorescent microscopy, and functional measurements of cell membrane anion permeability. Functional studies indicate that basal halide permeability is enhanced above control conditions following wild-type or ΔF508 NBD-1 expression in three different epithelial cell lines. Furthermore, when clinically relevant CFTR proteins truncated within NBD-1 (R553X or G542X) are expressed, surface localization and enhanced halide permeability are again established. Together, these findings suggest that isolated CFTR NBD-1 (with or without the ΔF508 mutation) is capable of targeting the epithelial cell membrane and enhancing cellular halide permeability. Furthermore, CFTR truncated at position 553 or 542 and possessing the majority of NBD-1 demonstrates surface localization and also confers increased halide permeability. These findings indicate that targeting to the plasma membrane and assumption of a transmembrane configuration are innate properties of the CFTR NBD-1. The results also support the notion that components of the halide-selective pore of CFTR reside within NBD-1.

The cystic fibrosis transmembrane conductance regulator or CFTR belongs to the traffic ATPase family, which includes numerous prokaryotic and eukaryotic proteins (*1*−*4*) that are generally involved in the transport of small molecules across the plasma membrane, including nutrients, mating factors, and chemotherapeutic agents. These proteins are characterized by conserved motifs, including (1) transmembrane (TM)[1] domains which are believed to be important in anchoring the proteins to the cell membrane and (2) nucleotide-binding domains (NBDs) that bind and hydrolyze ATP, providing the energy for substrate transport. CFTR also possesses a regulatory (R) domain that is predicted to be intracellular, contains multiple consensus phosphorylation sites for protein kinases A and C, and imparts phosphorylation-dependent regulation to the Cl^- conductive portion of the protein (*5*−*7*).

Many prokaryotic members of the traffic ATPase family are assembled as protein complexes, in which individual peptide domains (TMs and NBDs) are encoded by separate genes (*4*). Following translation, the individual components target the cell membrane, self-assemble, and produce a functioning traffic ATPase. Studies of several bacterial traffic ATPases have established that both TM and NBD motifs can traverse the prokaryotic cell membrane (*4*). The cellular localization of CFTR domains, however, remains

† Supported by Cystic Fibrosis Foundation Research Development Program, R464, Cystic Fibrosis Foundation Leroy Matthews Physicians/Scientist Award, CLANCY96LO, and NIH-NIDDK RO1 DK50831.

* Corresponding author: Phone: (205) 934-7210. Fax: (205) 934-7593.

‡ Department of Pediatrics.

§ Gregory Fleming James Cystic Fibrosis Research Center.

|| Department of Cell Biology.

⊥ Department of Medicine.

University of Nantes.

▽ Department of Microbiology.

[1] Abbreviations: CFTR, cystic fibrosis transmembrane conductance regulator; NBD-1, nucleotide-binding domain 1; ATP, adenosine triphosphate; TM, transmembrane; R, regulatory; wt, wild-type; SPQ, 6-methoxy-*N*-(3-sulfopropyl)quinolinium; AAV, adeno-associated virus; PMSF, phenylmethanesulfonylfluoride; IBMX, 3-isobutyl-1-methylxanthine; HEPES, *N*-(2-hydoxyethyl)piperazine-*N*′-(2-ethanesulfonic) acid; TPCK, *N*-tosyl-L-phenylalanine chloromethyl ketone; TLCK, *N*-P-tosyl-L-lysine chloromethyl ketone; LBTI, lima bean trypsin inhibitor; DMEM, Dulbecco's Modified Eagles' Media; FBS, fetal bovine serum; SDS, sodium dodecyl sulfate; PVDF, poly(vinylidene difluoride); NBT, 4-nitro blue tetrazolium chloride; BCIP, 5-bromo-4-chloro-3-indolyl-phosphate; MOI, multiplicity of infection; LacZ, gene encoding *β*-galactosidase; vT7, vaccinia virus encoding T7 polymerase; ORCC, outwardly rectified chloride channel.

10.1021/bi980436f CCC: $15.00
Published on Web 10/08/1998

controversial, specifically regarding the NBDs. Initial predictions of CFTR topology placed the NBDs strictly within the cell cytoplasm (*1*). More recent studies, however, suggest that CFTR NBD-1 might assume a transmembrane configuration, including studies demonstrating that (1) NBD-1 peptide interacts directly with membrane phospholipids and incorporates itself into liposomes (*8*, *9*), (2) anion conductive pores are formed by NBD-1 peptide in planar lipid bilayers (*10*), (3) CFTR NBD-1 is situated in a transmembrane configuration in *Escherichia coli* spheroplasts and retains the capacity to bind ATP in this setting (*11*), and (4) recombinant CFTR NBD-1 expressed in insect cells also assumes a transmembrane topology (*12*, *13*). To date, however, no direct examination of CFTR NBD-1 topology in mammalian cells has been performed.

In this study, we describe the behavior of CFTR NBD-1 following expression in three mammalian cell lines. Our findings indicate that NBD-1 targets the eukaryotic cell membrane, as determined by accessibility to extracellular protease digestion and biotinylation, confocal immunocytochemistry, and macroscopic effects on membrane permeability. Functional studies indicate that both wild-type (wt) NBD-1 and NBD-1 containing the ΔF508 mutation enhance basal cellular halide permeability. Expression of CFTR containing the clinically relevant mutations R553X or G542X, which each contain >70% of the NBD-1 motif, produce polypeptides that also target the cell membrane and enhance halide permeability in a manner similar to isolated NBD-1. These findings indicate that, like prokaryotic members of the traffic ATPase family, CFTR NBD-1 is capable of targeting the cell membrane and assuming a transmembrane configuration. The NBD-1 contains elements which enhance cellular halide permeability, and when clinically relevant CFTR mutations possessing the majority of NBD-1 are expressed, surface targeting and enhanced halide permeability are maintained.

EXPERIMENTAL PROCEDURES

Materials. Forskolin, NP-40, sodium deoxycholate, and PMSF were purchased from Calbiochem (San Diego, CA); IBMX, sodium iodide, sodium nitrate, magnesium nitrate, calcium nitrate, potassium nitrate, D-glucose, HEPES, mercaptoethanol, TPCK, TLCK, and LBTI were purchased from Sigma Biochemical (St. Louis, MO). Other reagents and their commercial sources were Biotin EZ-Link sulfo-NHS-biotin (Pierce Laboratories, Rockford, IL); SPQ (Molecular Probes, Eugene, OR); [^{35}S]methionine translabel (ICN, Costa Mesa, CA); chymotrypsin (Worthington Biochemicals, Freehold, NJ); SDS, Tris-Cl, polyacrylamide, and PVDF membranes (Bio-Rad Laboratories, Hercules, CA); alkaline phosphatase, tissue culture trays, DMEM, and Opti-MEM (Fisher Biotech, Pittsburgh, PA); NBT, BCIP, goat anti-rabbit antibody biotin conjugate, and polyclonal rabbit anti-β-galactosidase antibody (Boehringer Mannheim Corporation, Indianapolis, IN); FBS (Hyclone Laboratories, Logan, UT); rhodamine-tagged swine anti-rabbit antibody (DAKO Corporation, Carpinteria, CA); [^{35}S]streptavidin (Amersham Life Sciences, Arlington Heights, IL); protein G sepharose beads (Pharmacia Biotech, Uppsala, Sweden); and vectabond reagent (Vector Laboratories, Burlingame, CA). Neutralite avidin alkaline phosphatase conjugate was purchased from Southern Biotechnology Associates, Inc. (Birmingham, AL), and precast gels (10, 12, 14%, and density gradient) were purchased from Novex (San Diego, CA). Rabbit anti-human CFTR NBD-1 polyclonal antibody (raised against recombinant human NBD-1 amino acids 433−586) was produced as described (*14*). Mouse anti-human CFTR MATG-1031 monoclonal antibody was the generous gift of Dr. D. Escande (Nantes, France).

Vaccinia Viruses Expressing CFTR-Derived Constructs or β-Galactosidase. wtCFTR NBD-1 or CFTR NBD-1 containing the ΔF508 mutation was cloned into the *Nco*I site of the vaccinia expression vector pTF-EMC [pTF7−5 (*15*)] containing the EMC leader, provided by Dr. J. Engler, UAB. Briefly, DNA encoding the NBD-1 (aa 432−586 of full-length CFTR) was amplified from wtCFTR cDNA by PCR and the correct clones were verified by DNA sequencing of the inserts. Recombinant vaccinia viruses were generated according to published protocols (*16*). Recombinant vaccinia viruses containing wtCFTR and CFTR containing a premature stop codon at position 542 (G542X) or 553 (R553X) under the regulatory control of the T7 promoter was generated from constructs in the pTM1 vector (*15*) using standard techniques (*16*). Recombinant vaccinia virus expressing β-galactosidase was also generated by the described procedure after cloning the LacZ gene into pTF-EMC.

Methods. Vaccinia-Based Expression. Cells were infected with recombinant expression vectors at a MOI of 10 [5 MOI virus encoding construct with 5 MOI vTF7-3 (virus encoding T7 polymerase, referred to as vT7 throughout the remainder of this report) or 10 MOI of vT7 as a negative control] for 30 min in Opti-MEM at 37 °C, rinsed in PBS, and then returned to DMEM +10% FBS for 12−24 h until studied as indicated.

Chymotrypsin Digestion and Immunoprecipitation. COS-7 cells grown on 100 mm dishes were studied 12 h post infection. No cell damage was detected at this time point, as judged by inspection and the presence of functional CFTR activity in >75% of cells. Cells were washed with ice-cold PBS three times and then placed in 3 mL of PBS (pH 7.2) containing chymotrypsin (100 μg/mL) at 4 °C for 30 min (modified from ref *17*). Following incubation, cells were washed three times with ice-cold PBS containing a cocktail of protease inhibitors including LBTI (200 μg/mL), TPCK (70 μg/mL), TLCK (2 μg/mL), and PMSF (2 mM). The wash steps reduced the chymotrypsin levels ∼2500000-fold, while inhibitor levels (including the irreversible chymotrypsin inhibitors TPCK and PMSF) remained 1500−50 000 above the estimated chymotrypsin level at cell lysis. Cells were then lysed with RIPA buffer [NaCl 150 mM, NP-4O 1%, sodium-deoxycholate, 0.5%, SDS 0.1%, and Tris-Cl 50 mM (pH 8.0)] containing the protease inhibitor cocktail, and supernatant was immunoprecipitated with rabbit anti-NBD-1 polyclonal antibody (immunoprecipitation as in ref *18*). Proteins were separated on a 10% polyacrylamide gel, and electrophoretically transferred onto PVDF membranes. The membranes were washed with PBS + 0.1% tween three times, blocked with PBS + 0.1% tween + 1% BSA for 2 h, washed, incubated with rabbit anti-NBD-1 antibody (1:5000) for 2 h, washed, and incubated with biotinylated goat anti-rabbit conjugate (1:5000) for 2 h. Membranes were then washed and incubated with Neutralite avidin alkaline phosphatase conjugate (1:2000) for 2 h, and developed with

BCIP + NBT in carbonate buffer (pH 8.8) according to manufacturer's protocol (Boehringer Mannheim Corp.). Images were captured using the Eagle Eye II Imaging System (Stratagene) and analyzed with IPLab Spectrum software.

Cell Fractionation. COS-7 cells grown in 100 mM dishes expressing wtNBD-1, ΔF508 NBD-1, β-galactosidase, or vT7 (control) proteins without CFTR were washed in PBS and incubated in methionine-free DMEM for 1 h. Cells were then labeled with 100 μCi [^{35}S]methionine for 30 min. Incorporation was terminated by washing cells with PBS and replacing the media with nonradioactive DMEM (+methionine). Cells were then washed with PBS, scraped into ice-cold homogenation buffer (0.25 M sucrose, 10 mM acetic acid, 1 mM EDTA, pH 7.4, and protease inhibitors), and homogenized. Fractionation was performed as described by Wiertz *et al.* (*19*). Briefly, homogenates were centrifuged at 1000*g* for 10 min. Supernatants were then transferred and centrifuged at 10000*g* for 30 min, creating a particulate (membrane) fraction. Supernatants from the 10000*g* centrifugation were spun at 100000*g* for 60 min to clarify a cytosolic fraction. All pellets were washed with HEPES buffer (2.5 mM HEPES, pH 7.6, and 10 mM $CaCl_{l2}$), and then 500 μL of RIPA lysis buffer was added to each sample. After 30 min of lysis on ice, the samples were centrifuged at 14000*g* for 10 min. Immunoprecipitation, SDS−PAGE, immunoblotting, and phosphoimaging were performed as described below. Images were further characterized and densitometry was carried out using IPLab Spectrum software (Signal Analytics Corporation).

Biotinylation and Immunoprecipitation. COS-7 cells grown on 100 mm dishes were studied 12 h postinfection. Cells were washed with ice-cold PBS, and then placed in 3 mL of PBS (pH 7.2) containing NHS-biotin (500 μg/mL) at 23 °C for 30 min according to manufacturer's protocol (Pierce Laboratories, Rockford, IL). Following incubation, cells were washed three times with ice-cold PBS and then lysed with RIPA buffer. The lysate was immunoprecipitated with polyclonal rabbit anti-NBD-1 or rabbit anti-β-galactosidase. Proteins were separated and transferred to PVDF membranes as described above. The membranes were then washed with PBS + 0.1% tween, blocked with PBS + 0.1% tween + 1% BSA, washed, and then incubated with [^{35}S]-avidin (1.5 μCi) for 2 h. Membranes were washed, developed for 72 h on a phospho imaging screen (Molecular Dynamics), and analyzed with IPLab Spectrum software.

Immunoprecipitation of NBD-1, G542X, R553X, and wtCFTR. COS-7 cells grown in 6-well trays were infected with vT7 + vaccinia encoding CFTR constructs or vT7 alone as described above. For the studies of NBD-1, cells were lysed with RIPA buffer, immunoprecipitated with anti-NBD-1 antibody, and transferred to PVDF membranes. Detection was with rabbit anti-NBD-1 antibody (1:2000) probed with goat anti-rabbit biotin conjugate (1:5000). Development was with avidin alkaline phosphatase conjugate (1:2000), and NBT + BCIP in carbonate buffer, as above. For metabolic labeling, cells were incubated with translabel for 20 min using 250 μCi ^{35}S/mL at 12 h postinfection. Cells were lysed with RIPA buffer and proteins were separated by 12% SDS−PAGE. Proteins were transferred to PVDF membranes and then placed on a phosphoimaging screen for 24 h.

Digital Confocal Immunofluorescent Microscopy of COS-7 Cells Expressing wt or ΔF508 NBD-1. COS-7 cells grown on vectabond-treated glass coverslips transiently expressing wt or ΔF508 NBD-1 were studied 12 h after infection. Cells were formaldehyde fixed (4% methanol-free formalin diluted in PBS, pH 7.4) for 30 min, then underwent detergent permeabilization using 0.1% Triton X-100 in PBS at 23 °C for 10 min, and then were washed in PBS. The cells were treated with preimmune swine serum (1:20 dilution) in PBS for 20 min to block nonspecific protein-binding sites. CFTR NBD-1 antigen was detected using polyclonal rabbit anti-NBD-1 antibody (*20*). The secondary antibody was a rhodamine-tagged swine anti-rabbit antibody (DAKO). Cells were studied on an Olympus IX70 inverted reflective fluorescent light microscope at 623 nm excitation using UplanApo 100× or Uapo/340 40× objectives. Digital confocal images were captured using a Photometrics Sensys digital camera and analyzed with IPLab Spectrum software supplemented with Power Microtome extension software (Signal Analystics Corporation).

Digital Confocal Immunofluorescent Microscopy of COS-7 Cells Expressing wt or ΔF508 CFTR, G542X, or R553X. Cells were studied as above except that the detergent permeabilization step was omitted. Fixed cells were treated with 1:20 rabbit serum in PBS for 20 min. The monoclonal mouse anti-CFTR antibody, MATG-1031(1:20 dilution of ascites fluid), was applied to cells for 1 h at 23 °C (*21*). Cells were then washed with PBS, incubated with rhodamine-labeled anti-mouse IgG in blocking reagent for 40 min, washed, and mounted with Vectashield mounting medium. Images were captured and analyzed as above.

Anion Permeability Studies in Epithelial Cells. We performed studies of anion permeability in COS-7, C127 (murine breast), and $2CFSME_{0-}$ (CF human airway) cells (*7*, *22*, *23*). Briefly, cells were loaded for 10 min with the halide-sensitive dye SPQ by hypotonic shock (*24*, *25*) and mounted in a specially designed perfusion chamber for fluorescent measurements. Fluorescence of SPQ in single cells was measured with a Zeiss inverted microscope, a PTI digital imaging system, and a Hamamatsu camera as described previously (*26*). Excitation was at 340 nm, and emission was at >410 nm. All studies were performed at 37 °C. At the beginning of the experiments, cells were bathed in an iodide buffer to quench SPQ fluorescence. Following the establishment of a stable baseline fluorescence, cells were switched to a halide-free (nitrate) buffer, allowing dequench of SPQ. Fluorescence was normalized to the baseline (quenched) value, with increases shown as a percent increase over baseline (*25*). Fluorescent values reflect all dequenching cells studied from each condition.

Statistical Analysis. The slope of increasing normalized fluorescence over time from 200 to 600 s was tabulated for each cell type studied, and the slopes from each condition were compared by the Mann Whitney U test. *Z* coefficients were determined and converted to *P* values.

RESULTS

Expression of NBD-1 in Mammalian Epithelial Cell Lines. Figure 1A shows the detection of wtNBD-1 (amino acids 432−586) in three separate cell lines (C127i, COS-7, and $2CFSME_{0-}$) following vaccinia-based expression and sub-

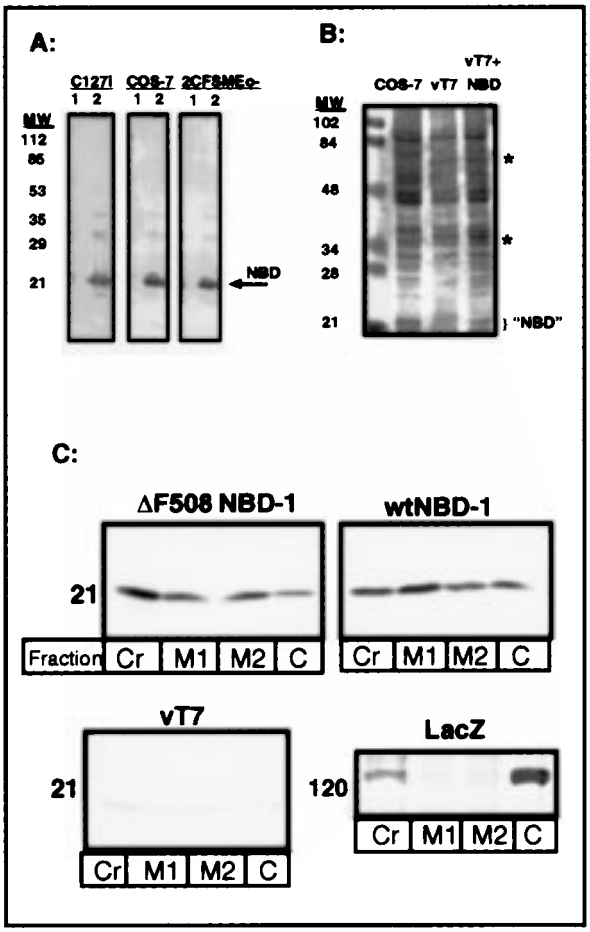

FIGURE 1: wtNBD-1 expression in epithelial cell lines. (A) Immunoblot of wtNBD-1 in three mammalian cell lines. Three cell lines (C127i, mouse mammary epithelioid; COS-7, simian kidney; $2CFSME_{0-}$, human CF respiratory) express wtNBD-1 following recombinant vaccinia infection. Lane 1 = lysate from control vaccinia virus (vT7) infected cells; lane 2 = lysate from NBD-1 expressing cells. Arrow indicates recombinant wtNBD-1 at the predicted size of ~21 kD. Over 75% of cells expressed detectable NBD-1 antigen, as assessed by immunohistochemistry (see Figure 4). (B) Total protein in COS-7 cell lysates. Cell lysates were separated by density gradient PAGE as described in the Experimental Procedures and stained with Coomassie blue (no immunoprecipitation). Lanes from left to right: molecular weight markers (MW), control (no vaccinia, COS-7), COS-7 cells with T7-vaccinia infection (vT7), COS-7 cells with vT7 and vaccinia encoding wtNBD-1 infection [vT7 (+) NBD]. Vaccinia-associated proteins could be detected in the vT7 and NBD-1 conditions (*). wtNBD-1 was expressed at low levels compared with other cellular or vaccinia-derived proteins, as (1) no wtNBD-1 specific protein band was identified near 21 kD (NBD), and (2) wtCFTR NBD-1 was detected only following immunoprecipitation of cell lysates (Figure 1A). (C) Fractionation of COS-7 cell homogenates. Cells expressing wtNBD-1, ΔF508 NBD-1, LacZ, or vT7 (control) proteins underwent homogenization, fractionation, and immunoprecipitation as described (ref *19* and Experimental Procedures). Lanes from left to right in each condition were 1000*g* pellet (crude pellet, Cr, unbroken cells and large debris), 10000*g* pellet (M1, particulate or membrane enriched fraction), 100000*g* pellet (M2, microsomes, small membrane debris, large protein complexes), and the remaining cytosolic supernatant (C). Densitometry was performed on the M1, M2, and C fractions. Approximately 80% of wtNBD-1 (M1 = 47%, M2 = 32%) and ΔF508 NBD-1 (M1 = 53%, M2 = 31%) localized to membrane fractions, while a minority localized to the cytosolic compartment (wtNBD-1, C = 21%; ΔF508 NBD-1, C = 16%). In contrast, >95% of the β-galactosidase protein localized to the cytosolic fraction, with minimal (<2%) of the protein localizing to membrane fractions. The vT7 control condition at 21kD is included for comparison to the NBD-1.

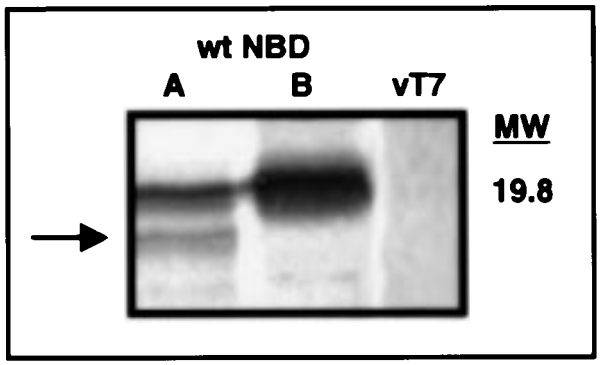

FIGURE 2: Chymotrypsin treatment of COS-7 cells expressing wtNBD-1. Cells expressing wtNBD-1 were exposed to 100 μg/mL chymotrypsin prior to cell lysis as described in the Experimental Procedures. Lane A = immunoprecipitated NBD-1 after chymotrypsin treatment, lane B = no chymotrypsin treatment. vT7 (negative) control following chymotrypsin treatment is also shown. A lower molecular weight band below wtNBD-1 (arrow) is identified and is unique to wtNBD-1 expressing cells treated with chymotrypsin.

sequent immunoprecipitation with a polyclonal anti-NBD-1 antibody (*20*, *27*). A recombinant protein of ~21 kDa was identified in each cell line. The level of expression of recombinant NBD-1 was modest compared with that of other endogenous cellular proteins. NBD-1 could not be detected as a major protein band when total cell lysates were examined by protein staining in the absence of Western blotting or immunoprecipitation (Figure 1B). In contrast, other (internal control) vaccinia-derived proteins that do not appear to influence anion permeability in these cells were expressed and easily identified (asterisks, Figure 1B). To initially characterize the cellular location of NBD-1 peptide, cell fractionation studies were performed comparing cells expressing wtNBD-1, ΔF508 NBD-1, and a control peptide (β-galactosidase). Figure 1C indicates that a majority (~80% of the homogenized fraction) of both wt and ΔF508 NBD-1 peptide localized to the particulate (membrane) fractions, in contrast to a control protein (LacZ; <2% recovery from particulate fraction). Together, these findings establish that (1) vaccinia-based expression of wtNBD-1 in mammalian cell lines produces detectable peptide, (2) the level of NBD-1 expression is lower than many other cellular proteins, either endogenous or vaccinia derived, and (3) NBD-1 peptide can be recovered from a membrane fraction of cellular homogenates.

Several studies suggest that isolated NBD-1 may associate with and/or traverse artificial, prokaryotic, and insect cell membranes. To determine whether isolated wtNBD-1 protein was detectable at the eukaryotic plasma membrane and accessible to extracellular modification, we performed a series of experiments in COS-7 cells following transient NBD-1 expression. Figure 2 compares the effects of extracellular chymotrypsin digestion in cells following vT7 or vT7/wtNBD-1 infection. Extracellular proteolysis produces low molecular weight peptides specifically after NBD-1 expression, which are absent in the vT7 condition, indicating accessibility of NBD-1 polypeptide to extracellular digestion. Figure 3 compares the effects of surface protein biotinylation by the membrane impermeant probe Biotin-X-NHS in cells following LacZ, wtNBD-1, or ΔF508 NBD-1 expression. A biotinylated peptide of ~21 kDa was identi-

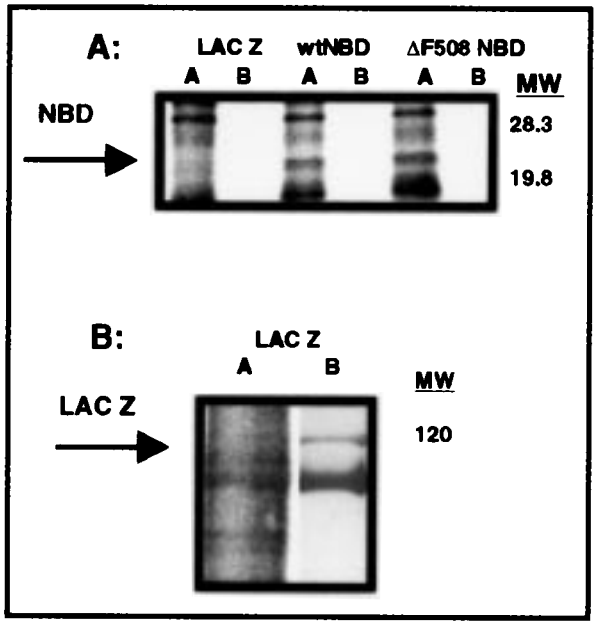

FIGURE 3: Surface protein biotinylation of COS-7 cells. Cells expressing LacZ, wtNBD-1, or ΔF508 NBD-1 were exposed to NHS-biotin (500 μg/mL) prior to cell lysis and immunoprecipitation as described in the Experimental Procedures. Lane A = presence of biotinylation, lane B = no biotinylation. (A) A ~21 kD protein is identified in both the wt and ΔF508 NBD-1 conditions following immunoprecipitation with anti-NBD-1 antibody (arrows) that is absent from the LacZ condition. (B) No biotinylated protein is identified at 120 kD in the LacZ condition following immunoprecipitation with anti-β-galactosidase antibody (arrow, lane A). β-galactosidase expression is confirmed by immunoblot of the same lane as described in the Experimental Procedures (lane B).

fied specifically after expression of wt or ΔF508 NBD-1. In contrast, no biotinylated LacZ-specific peptide was identified at either 21 kDa (Figure 3A) or 120 kDa (Figure 3B) from cells expressing β-galactosidase. The expression of β-galactosidase was confirmed by Western blotting (Figure 3B, Lane B). Although the efficiency of biotinylation was not directly measured in these studies, these results indicate that epitopes of NBD-1 are accessible for biotinylation from the extracellular surface. To further support these biochemical findings, we tested whether NBD-1 antigen was visibly detectable at the plasma membrane of cells expressing wtNBD-1 or ΔF508 NBD-1 using digital confocal immunofluorescent microscopy. For these experiments, we used a polyclonal rabbit anti-NBD-1 antibody which has been validated previously by its ability to (1) immunoprecipitate either truncated or full-length CFTR from several cell types, (2) immunolocalize CFTR to cells overexpressing the protein, and (3) correctly identify the presence or absence of CFTR in vivo from salivary gland sections of wild-type or CFTR knockout mice of the same strain (*14*, *20*, *28*). Figure 4 demonstrates a plasma membrane staining pattern in cells expressing wtNBD-1 (panel A) or ΔF508 NBD-1 (panel B), while vT7 control cells exhibited no detectable antigen (panel C). Together, these results indicate that NBD-1 expression produces peptide which is capable of localizing to and traversing the mammalian plasma membrane.

At least two studies suggest that components of NBD-1 are capable of forming halide and other anion conductive pores (*10*, *28*). To determine whether NBD-1 influences halide permeability in epithelial cells, we compared the

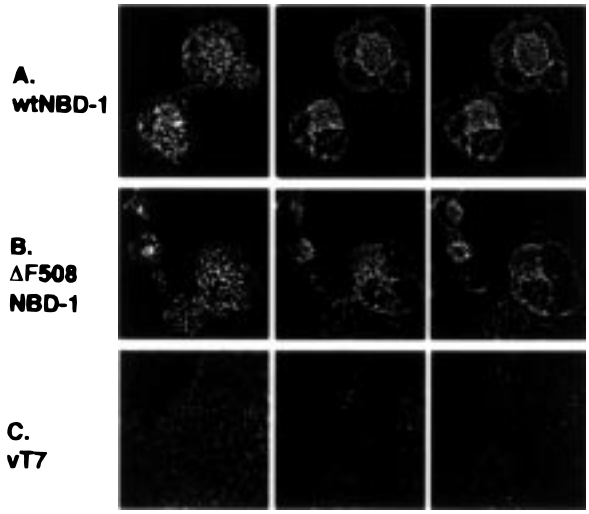

FIGURE 4: Immunolocalization of wtNBD-1 and ΔF508 NBD-1 in COS 7 cells. Cells were grown on glass coverslips, infected with vT7 alone, or vT7 with vaccinia encoding wt or ΔF508 NBD-1 and studied by confocal microscopy. A polyclonal antibody was used to localize the NBD-1 polypeptide (*20*). Panels from left to right are descending cross sections through cells (40X). Panel A = wtNBD-1, panel B = ΔF508 NBD-1, panel C = vT7 control cells. Note the increased fluorescence in the superior sections and the cell periphery. More than 75% of cells in the wt and ΔF508 NBD-1 conditions had detectable NBD-1 antigen.

effects of NBD-1 expression on basal halide permeability as measured by SPQ fluorescence in three epithelial cell lines. SPQ is a well established measure of regulated and unregulated halide efflux in transient vaccinia-based expression systems, and has been used extensively to characterize wt and mutant CFTR function (*6*, *7*, *30*−*33*). The results from Figure 5 indicate that NBD-1 expression increases basal halide permeability above that of vT7 infected cells in all three cell lines tested, with increases above control conditions ranging 2−5-fold. Furthermore, both wtNBD-1 and ΔF508 NBD-1 had similar effects on halide permeability in the two cell lines tested (COS-7 and C127i). In no cell line was basal halide permeability further enhanced following stimulation with cAMP (20 μM forskolin + 100 μM IBMX) or ionomycin (2 μM, data not shown). COS-7 cells expressing wtCFTR stimulated with cAMP (20 μM forskolin + 100 μM IBMX) are included for comparison (Figure 5B).

Expression of R553X and G542X CFTR in Mammalian Epithelial Cell Lines. The studies described above demonstrate that isolated NBD-1 is capable of targeting the epithelial plasma membrane, assuming a transmembrane configuration, and enhancing basal cellular halide permeability. We next asked whether mutant CFTRs which include significant portions of NBD-1 but lack distal (carboxy) domains were also capable of plasma membrane localization and function. We chose to study two clinically relevant mutant CFTR molecules possessing premature stop codons, G542X and R553X. These mutations are found in approximately 5% of the CF population (*34*) and include 72% (G542X) to 79% (R553X) of the NBD-1 (aa 432−586). Figure 6 shows detection of ^{35}S-labeled truncated proteins [~53 kDa (G542X); ~55 kDa (R553X)] from COS-7 cell lysates following vaccinia-based expression. Full-length CFTR is shown for comparison. No full-length CFTR is detected in cells expressing either of the mutant cDNAs. To determine whether these truncated proteins were capable of

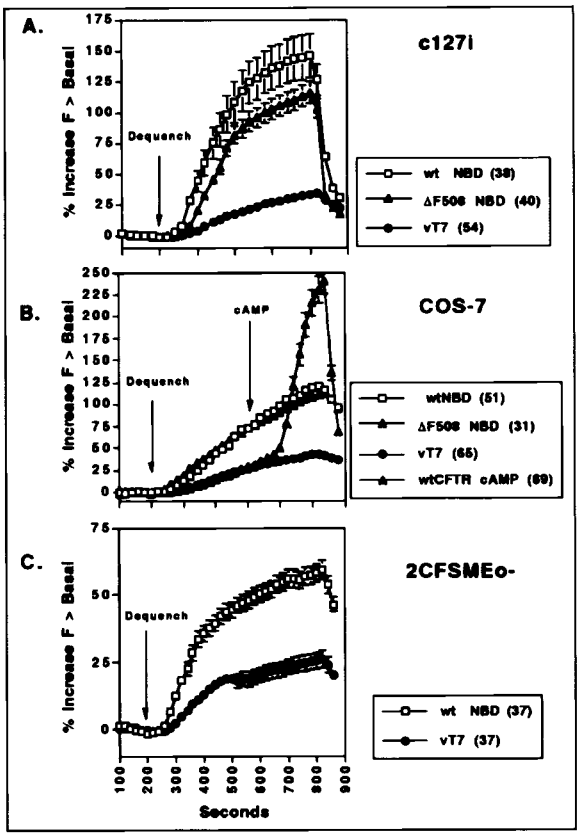

FIGURE 5: NBD-1 expression increases halide permeability in three mammalian cell lines. In each of the three cell lines (A = c127i; B = COS-7; C = 2CFSME$_{0-}$), wtNBD-1 (open squares) induced an increased rate of dequench above the vT7 infected controls (closed circles), corresponding to an increased halide permeability. In no paired experiment did the vT7 controls achieve a dequench greater or equal to the NBD-1 condition. The number in parentheses represents the total number of cells included in the presented curve. In the two cell lines tested (c127i and COS-7), the wt and ΔF508 NBD-1 (black triangles) curves revealed similar dequench which was greater than the vT7 condition ($P < 0.0001$ for wtNBD-1 and ΔF508 NBD-1 compared with vT7 alone in each cell line tested). The effects of wtCFTR on basal and regulated permeability (cAMP-stimulation with 20 μM forskolin + 100 μM IBMX at 500 s) in COS-7 cells is shown for comparison in Figure 5B (gray triangles, rapid dequench following cAMP).

plasma membrane localization, we performed digital confocal immunofluorescent microscopy using the monoclonal MATG-1031 antibody. This antibody recognizes an epitope in the first predicted extracellular loop of CFTR TM-1, which is shared by wtCFTR, R553X, and G542X. MATG-1031 has been used to identify surface-localized CFTR in stable cell lines and native respiratory epithelia (*21*). Cells were studied with and without detergent permeabilization. Figure 7 indicates a plasma membrane staining pattern in cells without detergent permeabilization following wtCFTR, R553X, and G542X expression, but not ΔF508 CFTR. In contrast, all conditions revealed detectable antigen following detergent permeabilization (for example, as shown for ΔF508 CFTR, Figure 7C). These studies provide evidence of plasma membrane targeting by CFTR possessing either the G542X or R553X mutations.

To determine whether either R553X or G542X CFTR had positive effects on basal cellular halide permeability, we performed SPQ analysis in COS-7 cells expressing these mutant cDNAs (Figure 8). The truncated CFTR proteins

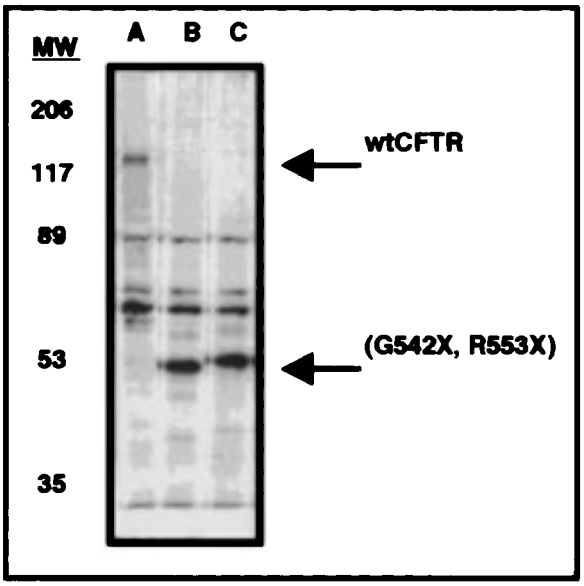

FIGURE 6: Immunoblot of wt, R553X, and G542X CFTR in COS-7 cells. Cells were labeled with translabel for 20 min at 12 h after infection and immunoprecipitated with anti-NBD-1 antibody as described in the Experimental Procedures. Lane A = wtCFTR, lane B = G542X, lane C = R553X.

enhanced basal halide permeability above control cells expressing vaccinia proteins (vT7) or cells with vaccinia-based expression of LacZ. Stimulation with cAMP (20 μM forskolin + 100 μM IBMX) failed to produce regulated halide permeability. The effects of R553X, G542X, and NBD-1 on COS-7 cell basal halide permeability were qualitatively and quantitatively similar (compare with Figure 5B).

DISCUSSION

In the present experiments, NBD-1 expression in mammalian cells led to readily detectable NBD-1 levels in the particulate (membrane) fraction of cell homogenates (Figure 1C), plasma membrane localization of the peptide (Figures 2, 3, and 4), and a transmembrane configuration as judged by two different biochemical assays (extracellular proteolysis and surface biotinylation, Figures 2 and 3). Plasma membrane targeting by NBD-1 was associated with an increase in basal halide permeability in three mammalian epithelial cell lines (Figure 5). Previous studies from our laboratory and others have indicated that the CFTR NBD-1 (1) is highly lipophilic, fusing with and disrupting liposomes and other artificial membranes in vitro (*8*, *9*), (2) traverses the prokaryotic cell membrane with retention of ATP binding capacity (*11*), (3) is accessible to extracellular labeling in an insect cell system (*12*, *13*), and (4) forms an anion pore after reconstitution into planar lipid bilayers (*10*). A peptide corresponding to 30 amino acids within NBD-1 (amino acid 477−508) behaves similarly to the complete NBD-1 in the planar lipid bilayer, conducting halides and other anions (*29*). Additionally, isolated prokaryotic NBDs from closely related members of the traffic ATPase family such as HisP, OPP D, and F, P29, and malK target the prokaryotic cell membrane (*4*, *35*−*38*). At least two (HisP and malK) have been shown to assume a transmembrane configuration (*35*, *36*). Our results demonstrate that this property is retained by isolated CFTR NBD-1 when expressed in eukaryotic cells.

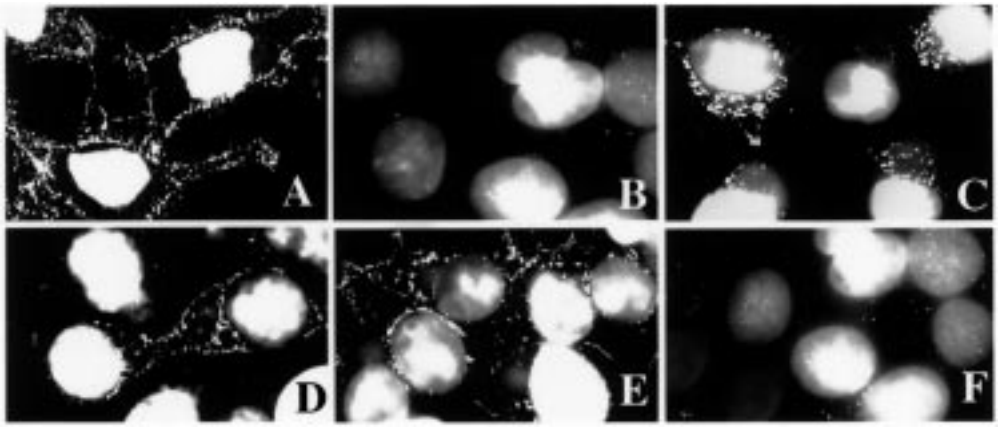

FIGURE 7: Localization of wtCFTR, R553X, and G542X to the cell surface in COS-7 cells by confocal immunocytochemistry. Cells were studied by confocal microscopy using the monoclonal anti-CFTR antibody MATG-1031. Panels from left to right are cross sections of cells at the level of the nucleus and cell surface membrane, without and with detergent permeabilization (40X) as indicated. Upper panels from left to right are (A) wtCFTR without permeabilization, (B) ΔF508 CFTR without permeabilization, and (C) ΔF508 CFTR with permeabilization. Lower panels from left to right are (D) G542X without permeabilization, (E) R553X without permeabilization, and (F) vT7 controls with permeabilization.

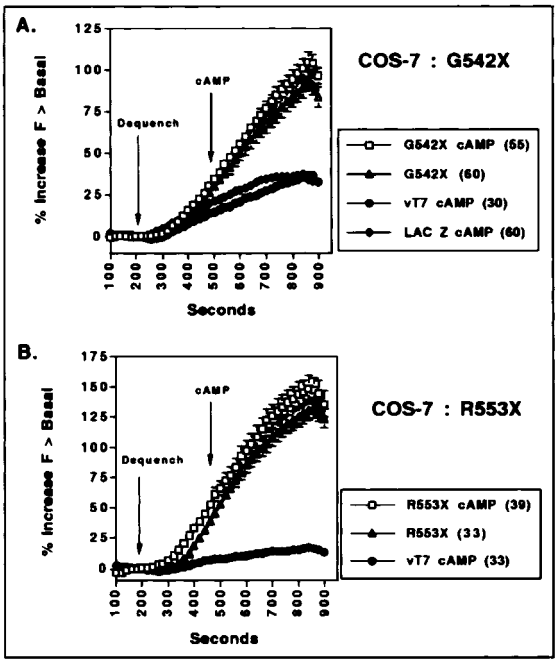

FIGURE 8: R553X or G542X expression increases halide permeability in COS-7 cells. Cells grown on glass coverslips were studied by SPQ as in Figure 5. Cells expressing truncated CFTR with (open squares) and without (triangles) cAMP stimulation (20 μM forskolin + 100 μM IBMX at 500 s) are compared with vT7 (closed circles) and LacZ (gray diamonds) infected cells stimulated with cAMP. The numbers in parentheses are the total number of cells included in each curve. (A) Dequench of the G542X expressing cells was significantly elevated above control cells ($P < 0.0001$ compared with vT7 or LacZ conditions). (B) Dequench of the R553X expressing cells was significantly elevated above controls ($P < 0.0001$ compared with vT7 expressing cells).

This result has significance, since modeling of the CFTR NBDs based on the amino acid sequence has suggested a cytoplasmic localization for the domain (*1*, *2*). Our data indicates a tendency for the NBD-1 portion of CFTR to span the mammalian epithelial plasma membrane.

Expression of truncated CFTR (R553X CFTR and G542X CFTR, Figures 6, 7, and 8) produces a protein which also targets the eukaryotic plasma membrane, enhancing cellular basal halide permeability. Neither R553X nor G542X produces cAMP-regulated halide permeability, and no full-length CFTR could be detected by immunoprecipitation, indicating that suppression of the premature termination codons is not responsible for the ion transport results shown here (*39*, *40*). The enhanced basal halide permeability conferred by R553X and G542X is qualitatively and quantitatively similar to that produced by NBD-1 (Figure 5). We suggest that the truncated CFTR proteins G542X and R553X contain adequate domains and the appropriate cellular signals to fold into functional peptides and localize to the cell membrane. The common halide permeability enhancing effects produced by G542X, R553X, and isolated NBD-1 suggest that these three polypeptides share common amino acids (422−542 of the complete CFTR molecule) which may be able to activate halide permeability in several epithelial cell types.

On the basis of the findings that R553X and G542X retain surface localizing and residual halide transport function, we recently studied five patients possessing at least one of these alleles, but found no evidence of residual Cl^- secretion during a nasal potential difference protocol (*25*). We attributed the absence of Cl^- secretion in vivo to instability of CFTR mRNA possessing premature stop codons, which has been reported to reduce the levels of truncated CFTR protein product (*41*, *42*). Interestingly, a tendency toward decreased Na^+ transport compared with ΔF508 homozygote controls was observed in the nasal airways of these patients and is consistent with the finding that the CFTR truncated at position 553 retains the ability to downregulate Na^+ transport in an oocyte expression system (*43*). Further studies in a larger number of CF patients will be necessary in order to establish improvements in the CF Na^+ transport abnormality conferred by CFTR truncation alleles. In either case, our results clearly establish that, unlike class II CFTR mutations (*34*), R553X and G542X CFTR are capable of escaping intracellular degradation, targetting the plasma membrane, and forming functional proteins that maintain some residual halide transport function. These properties might be utilized in new approaches to CF therapy, if methods for increasing CFTR mRNA or truncated protein stability could be developed (*44*, *45*).

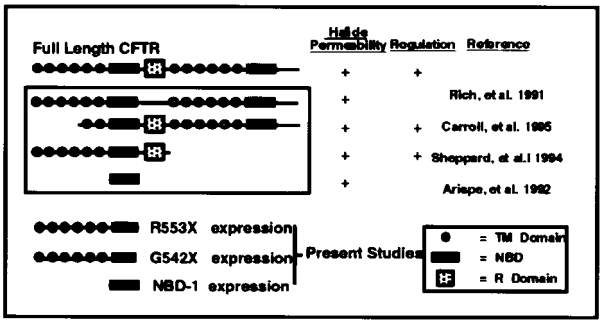

FIGURE 9: Summary of studies concerning assignment of CFTR pore-forming elements to defined domains. The figure to the left summarizes CFTR constructs previously evaluated, while the accompanying table provides information regarding halide permeability and presence or absence of regulation (see text).

Expression studies following deletion of CFTR domains have been informative regarding the constituents of CFTR that regulate Cl^- conduction. Flotte et al. observed that CFTR expressed from an AAV vector functioned normally even when the first predicted membrane-spanning α-helix (residues 1−119 of CFTR) was omitted (*46*). Carroll et al. subsequently showed that omission of the first four predicted membrane-spanning α-helices (i.e., a CFTR beginning at residue 265) maintained an anion-selective pore similar to that observed in the wild-type CFTR (*47*). These studies of transmembrane segment deletion could suggest that earlier studies of point mutations in TM segments 1 and 6 (which led to altered CFTR anion selectivity, suggesting a contribution of these alpha helices to the CFTR Cl^- conductive pore) might be describing effects at a distance, i.e., raising the possibility that some of these transmembrane segment point mutations were not within the Cl^- pore itself (*32*, *48*). On the other hand, Sheppard et al. have demonstrated that a truncated CFTR molecule containing TM-1, NBD-1, and the R domain (D836X) remains capable of forming anion-selective channels with phosphorylation-dependent regulation (*49*). This result indicated that all elements necessary for CFTR Cl^- channel assembly could be found in the first 836 amino acids of CFTR. In earlier studies, Rich et al. showed that deletion of CFTR amino acids 708−835 (ΔRCFTR, i.e., CFTR lacking a portion of the R domain) did not obliterate the pore-forming activity of CFTR but, instead, led to the predicted absence of phosphorylation-dependent activation (*6*). A summary of these results, together with our current findings, is presented in Figure 9. Note that all CFTR constructs reported to maintain anion channel activity contain the majority of NBD-1.

The actual residues lining the anion-selective pore within CFTR are controversial. In Figure 9, we have focused on mutations which lead to active Cl^- channels, since this sort of information provides a very stringent criterion by which to judge the possible location of the pore. Mutations that lead to subtle alteration or even complete loss of Cl^- channel activity are difficult to interpret since even a point mutations may disrupt channel function by inducing defects in overall CFTR protein folding, influencing pore function from a distance (*7*, *34*, *50*). For example, the finding by Welsh and colleagues that CFTR without the NBD-1 is processed normally, but loses the ability to mediate Cl^- permeability, is consistent with the hypothesis that NBD-1 contains pore-forming elements (*33*). However, the absence of an active Cl^- pore is only partially informative, since there are many ways in which a deletion of this sort might disrupt protein folding or pore formation, irrespective of the physical location of the Cl^- pore. As another example, Akabas and colleagues recently demonstrated that covalent modification of residues in either α-helix 1 or 6 led to decreased ion conductance by CFTR and concluded that these two regions contributed to the lining of an anion-selective pore. The authors noted that covalent labeling did not formally rule out effects on pore function at a distance, although the data provided clear evidence that residues within α-helices 1 and 6 are accessible to the extracellular environment (*51*, *52*). Nevertheless, this important series of experiments does not explain previous studies of CFTR indicating intact function even in the complete absence of the first α-helix (*46*, *47*). Interestingly, amino acid substitutions at position 338 of CFTR, which has been predicted to contribute to the peptide backbone of the CFTR Cl^- channel and not line the channel itself (*52*), altered the anion selectivity series of the CFTR anion channel (*53*). This finding suggests that indeed single amino acid substitutions at sites removed from the predicted halide conductive portion of CFTR may have effects on the single-channel properties of CFTR. Our present results establish surface localization, a transmembrane configuration, and enhancement of halide permeability by NBD-1 in living epithelial cells and provide important support for the previous finding that anion pore function exists within NBD-1 of the overall CFTR molecule (*10*, *28*, *29*).

ACKNOWLEDGMENT

We are indebted to Jan Tidwell and Kynda Roberts for her help preparing this manuscript and Dr. Cathy Fuller for her critical review. We are also grateful to Kevin Hicks for technical assistance. J.P.C. is a Cystic Fibrosis Foundation Leroy Matthews Physicians/Scientist award recipient.

REFERENCES

1. Hyde, S. C., Emsley, P., Hartshorn, M. J., Mimmack, M. M., Gileadi, U., Pearce, S. R., Gallagher, M. P., Gill, D. R., Hubbard, R. E., and Higgins, C. F. (1990) *Nature 346*, 362−365.
2. Riordan, J. R., Rommens, J. M., Kerem, B. T., Alon, N., Rozmahel, R., Grzelczak, Z., Zielenski, J., Lok, S., Plavsic, N., Chou, J. L., Drumm, M. L., Iannuzzi, M. C., Collins, F. S., and Tsui, L.-C. (1989) *Science 245*, 1066−1073.
3. Mimura, C. S., Holbrook, S. R., and Ames, G. F.-L. (1991) *Proc. Natl. Acad. Sci. U.S.A.* 88, 84−88.
4. Doige, C. A., and Ames, G. F. (1993) *Annu. Rev. Microbiol. 47*, 291−319.
5. Berger, H. A., Travis, S. M., and Welsh, M. J. (1993) *J. Biol. Chem. 268*, 2037−2047.
6. Rich, D. P., Gregory, R. J., Anderson, M. P., Manavalan, P., Smith, A. E., and Welsh, M. J. (1991) *Science 253*, 205−207.
7. Cheng, S. H., Rich, D. P., Marshall, J., Gregory, R. J., Welsh, M. J., and Smith, A. E. (1991) *Cell 66*, 1027−1036.
8. Bar-Noy, S., McPhie, P., Lee, G., Huang, Z., Sorscher, E. J., Eidelman, O., and Pollard, H. B. (1996) *Ped. Pulmon. Suppl. 13*, 213 (Abstr. 17).
9. Lee, G., Cohen, B. E., BarNoy, S., Eidelman, O., Jacobson, K. A., and Pollard, H. B. (1995) *Ped. Pulmon. Suppl. 12*, 185 (Abstr. 23).
10. Arispe, N., Rojas, E., Hartman, J., Sorscher, E. J., and Pollard, H. (1992) *Proc. Natl. Acad. Sci. U.S.A. 89*, 1539−1543.
11. Ko, Y. H., Delannoy, M., and Pedersen, P. L. (1997) *Biochemistry 36*, 5053−5064.

12. Gruis, D. B., Franke, K. E., and Price, E. M. (1995) *Pediatr. Pulmon. Suppl. 12*, 180 (Abstr. 6).
13. Gruis, D. B., and Price, E. (1997) *Biochemistry 36* (25), 7739−7745.
14. Peng, S., Sommerfelt, M., Logan, J., Huang, Z., Jilling, T., Kirk, K., Hunter, E., and Sorscher, E. J. (1993) *Protein Expression Purif. 4*, 95−100.
15. Moss, B., Elroy-Stein, O., Mizukami, T., Alexander, W. A., and Fuerst, T. R. (1990) *Nature 348*, 91−92.
16. Springer, T. A. (1994) in *Short Protocols in Molecular Biology* (Ausubel, F. M., Brent, R., Kingston, R. E., Moore, D. D., Seidman, J. G., and Smith, J. A., Eds.) pp 10.16.1−10.16.11, John Wiley & Sons, Inc., New York.
17. Steck, T. L., Ramos, B., and Strapazon, E. (1976) *Biochemistry 15* (5), 1154−1161.
18. Cheng, S. H., Gregory, R. J., Marshall, J., Paul, S., Souza, D. W., White, G. A., O'Riordan, C. R., and Smith, A. E. (1990) *Cell 63*, 827−834.
19. Wiertz, E. J. H. J., Jones, T. R., Sun, L., Bogyo, M., Genze, A., and Ploegh, H. L. (1996) *Cell 84*, 769−779.
20. Hasty, P., O'Neal, W. K., Liu, Q., Morris, A. P., Bebok, Z., Shumyatsky, G. B., Jilling, T., Sorscher, E. J., Bradley, A., and Beaudet, A. L. (1995) *Somatic Cell Mol. Genet. 21*, 177−187.
21. Demolombe, S., Baró, I., Bebok, Z., Clancy, J. P., Sorscher, E. J., Thomas-Soumarmon, A., Pavirani, A., and Escande, D. (1996) *Gene Ther. 3*, 685−694.
22. Marshall, J., Fang, S., Ostedgaard, L. S., O'Riordan, C. R., Ferrara, D., Amara, J. F., Hoppe, H., Scheule, R. K., Welsh, M. J., Smith, A. E., and Cheng, S. H. (1994) *J. Biol. Chem. 269*, 2987−2995.
23. Bebok, Z., Abai, A. M., Dong, J.-Y., King, S. A., Kirk, K. L., Berta, G., Hughes, B. W., Kraft, A. S., Burgess, S. W., Shaw, W., Felgner, P. L., and Sorscher, E. J. (1996) *J. Pharmacol. Exp. Ther. 279* (3), 1462−1469.
24. Verkman, A. S. (1990) *Am. J. Physiol. 259* (Cell Physiol.), C375−C388.
25. Walker, R. C., Venglarik, C. J., Aubin, G., Weatherly, M. R., McCarty, N. A., Lesnick, B., Ruiz, F., Clancy, J. P., and Sorscher, E. J. (1997) *Am. J. Res. Crit. Care Med. 155*, 1684−1689.
26. Sorscher, E. J., Kirk, K., Weaver, M. L., Jilling, T., Blalock, J. E., and LeBouef, R. D. (1991) *Proc. Natl. Acad. Sci. U.S.A. 88*, 7759−7762.
27. Hartman, J., Huang, Z., Rado, T. A., Peng, S., Jilling, T., Muccio, D. D., and Sorscher, E. J. (1992) *J. Biol. Chem. 267*, 6455−6458.
28. Clancy, J. P., Hong, J., Bebok, Z., King, S., Demolombe, S., Escande, D., Howard, M., and Sorscher, E. J. (1995) *Ped. Pulmon. Suppl. 12*, Late Breaking Science (Abstr.).
29. Arispe, N., Lee, G., Bar-Noy, S., McPhie, P., and Pollard, H. B. (1996) *Ped. Pulmon. Suppl. 13*, 216 (Abstr. 28).
30. Anderson, M. P., Rich, D. P., Gregory, R. J., Smith, A. E., and Welsh, M. J. (1991) *Science 251*, 679−682.
31. Gregory, R. J., Rich, D. P., Cheng, S. H., Souza, D. W., Paul, S., Manavalan, P., Anderson, M. P., Welsh, M. J., and Smith, A. E. (1991) *Mol. Cell Biol. 11*, 3886−3893.
32. Anderson, M. P., Gregory, R. J., Thompson, S., Souza, D. W., Paul, S., Mulligan, R. C., Smith, A. E., and Welsh, M. J. (1991) *Science 253*, 202−205.
33. Rich, D. P., Gregory, R. J., Cheng, S. H., Smith, A. E., and Welsh, M. J. (1993) *Receptors and Channels*, pp 221−232, Harwood Academic Publishers.
34. Welsh, M. J., Tsui, L., Boat, T. F., and Beaudet, A. L. (1995) in *The Metabolic and Molecular Bases of Inherited Disease* (Scriver, C. R., Beaudet, A. L., Shy, W. S., and Valle, D., Eds.) pp 3799−3876, McGraw-Hill, Inc., New York.
35. Schneider, E., Hunke, S., and Tebbe, S. (1995) *J. Bacteriology 177* (18), 5364−5367.
36. Baichwal, V., Liu, D, and Ames, G. F.-L. (1993) *Proc. Natl. Acad. Sci. U.S.A. 90*, 620−624.
37. Dudler, R., Schmidhauser, C., Parish, R. W., Wettenhall, R. E. H., and Schmidt, T. (1988) *EMBO J. 7* (12), 3963−3970.
38. Hiles, I. D., Gallagher, M. P., Jamieson, D. J., and Higgins, C. F. (1987) *J. Mol. Biol. 195*, 125−142.
39. Bedwell, D. M., Kaenjak, A, Benos, D. J., Bebok, Z., Bubien, J. K., Hong, J., Tousson, A., Clancy, J. P., and Sorscher, E. J. (1997) *Nat. Med. 3* (11), 1280−1284.
40. Howard, M., Frizzell, R. A., and Bedwell, D. M. (1995) *Nat. Med. 2*, 467−469.
41. Hamosh, A., Trapnell, B. C., Zeitlin, P. L., Montrose-Rofizadeh, C., Rosenstein, B. J., Crystal, R. G, and Cutting, G. R. (1991) *J. Clin. Invest. 88* (6), 1880−1885.
42. Hamosh, A., Rosenstein, B. J., and Cutting, G. R. (1992) *Hum. Mol. Genet. 1*, 542−544.
43. Awayda, M. S., and Benos, D. J. (1996) *Ped. Pulmon. Suppl. 13*, 233 (Abstr. 88).
44. Cheng, S. H., Fang, S. L., Zabner, J., Marshall, J., Piraino, S., Schiavi, S. C., Jefferson, D. M., Welsh, M. J., and Smith, A. E. (1995) *Am. J. Physiol. 268*, L615−L624.
45. Rubenstein, R. C., Egan, M. E., and Zeitlin, P. L. (1997) *J. Clin. Invest. 100* (10), 2457−2465.
46. Flotte, T. R., Afione, S. A., Conrad, C., McGrath, S. A., Solow, R., Oka, H., Zeitlin, P. L., Guggino, W. B., and Carter, B. J. (1993) *Proc. Natl. Acad. Sci. U.S.A. 90*, 10613−10617.
47. Carroll, T. P., Morales, M. M., Fulmer, S. B., Allen, S. S., Flotte, T. R., Cutting, G. R., and Guggino, W. B. (1995) *J. Biol. Chem. 270*, 11941−11946.
48. Tabcharani, J. A., Rommens, J. M., Hou, Y. X., and Chang, X. B. (1993) *Nature 366*, 79−82.
49. Sheppard, D. N., Ostedgaard, L. S., Rich, D. P., and Welsh, M. J. (1994) *Cell 76*, 1091−1098.
50. Hwang, T. C. (1997) *Ped. Pulmon. Suppl. 14*, 243 (Abstr. 124).
51. Akabas, M. H., Kaufmann, C., Cook, T. A., and Archdeacon, P. (1994) *J. Biol. Chem. 269* (21), 14865−14868.
52. Cheung, M., and Akabas, M. H. (1996) *Biophy. J. 70*, 2688−2695.
53. Linsdell, P., Zheng, S.-X., and Hanrahan, J. W. (1997) *Ped. Pulmon. Suppl. 14*, 214 (Abstr. 15).

BI980436F